

UC Berkeley

UC Berkeley Previously Published Works

Title

Comprehensive genomic and transcriptomic analysis of polycyclic aromatic hydrocarbon degradation by a mycoremediation fungus, *Dentipellis* sp. KUC8613

Permalink

<https://escholarship.org/uc/item/3k89v3s1>

Journal

Applied Microbiology and Biotechnology, 103(19)

ISSN

0175-7598

Authors

Park, Hongjae
Min, Byoungnam
Jang, Yeongseon
et al.

Publication Date

2019-10-01

DOI

10.1007/s00253-019-10089-6

Peer reviewed

1 **Comprehensive Genomic and Transcriptomic Analysis of**
2 **Polycyclic Aromatic Hydrocarbon Degradation by a**
3 **Mycoremediation Fungus, *Dentipellis* sp. KUC8613**

4
5 Hongjae Park^a, Byoungnam Min^b, Yeongseon Jang^c, Jungyeon Kim^j, Anna
6 Lipzen^b, Aditi Sharma^b, Bill Andreopoulos^b, Jenifer Johnson^b, Robert Riley^b,
7 Joseph W. Spatafora^d, Bernard Henrissat^{e,f,g}, Kyoung Heon Kim^j, Igor V.
8 Grigoriev^{b,i}, Jae-Jin Kim^h, and In-Geol Choi^{1,*}

9
10 *^aDepartment of Biotechnology, College of Life Sciences and Biotechnology,*
11 *Korea University, Seoul 02841, Korea, ^bUS Department of Energy Joint*
12 *Genome Institute, 2800 Mitchell Drive, Walnut Creek, CA 94598, United*
13 *State, ^cDivision of Wood Chemistry & Microbiology, Korea Forest Research*
14 *Institute, Seoul, 130-712, Korea, ^dDepartment of Botany and Plant*
15 *Pathology, Oregon State University, Corvallis, OR 97331-2902, United*
16 *States, ^eArchitecture et Fonction des Macromolécules Biologiques, Centre*
17 *National de la Recherche, France, ^fScientifique, Université d'Aix-Marseille,*
18 *France, Institut National de la Recherche Agronomique, USC 1408 AFMB,*
19 *Marseille, France, ^gDepartment of Biological Sciences, King Abdulaziz*
20 *University, Jeddah, Saudi Arabia, ^hDivision of Environmental Science and*
21 *Ecological Engineering, College of Life Sciences and Biotechnology, Korea*
22 *University, Seoul 02841, ⁱDepartment of Plant and Microbial Biology,*
23 *University of California - Berkeley, Berkeley, 111 Koshland Hall, Berkeley,*
24 *CA 94720, ^jDepartment of Biotechnology, Graduate School, Korea*
25 *University, Seoul, 02841, South Korea*

26
27
28 * Corresponding author:

29 In-Geol Choi

30 Tel.: +82-2-3290-3152, E-mail address: igchoi@korea.ac.kr

31

33 **Abstract**

34 The environmental accumulation of polycyclic aromatic
35 hydrocarbons (PAHs) is of great concern due to potential carcinogenic and
36 mutagenic risks, as well as their resistance to remediation. While many
37 fungi have been reported to break down PAHs in environments, the details
38 of gene-based metabolic pathways are not yet comprehensively
39 understood. Specifically, the genome-scale transcriptional responses of
40 fungal PAH-degradation have rarely been reported. In this study, we report
41 the genomic and transcriptomic basis of PAH-bioremediation by a potent
42 fungal degrader, *Dentipellis* sp. KUC8613. The genome size of this fungus
43 was 36.71 Mbp long encoding 14,320 putative protein-coding genes. The
44 strain efficiently removed more than 90 % of 100 mg/liter concentration of
45 PAHs within ten days. The genomic and transcriptomic analysis of this
46 white rot fungus highlights that the strain primarily utilized non-
47 ligninolytic enzymes to remove various PAHs, rather than typical
48 ligninolytic enzymes known for playing important roles in PAH-
49 degradation. PAH-removal by non-ligninolytic enzymes was initiated by
50 both different PAH-specific and common overexpression of P450s, followed
51 by downstream PAH-transforming enzymes such as epoxide hydrolases,
52 dehydrogenases, FAD-dependent monooxygenases, dioxygenases and
53 glycosyl- or glutathione transferases. Among the various PAHs,
54 phenanthrene induced a more dynamic transcriptomic response possibly
55 due its greater cytotoxicity, leading to highly upregulated genes involved
56 in the translocation of PAHs, a defense system against reactive oxygen
57 species, and ATP synthesis. Our genomic and transcriptomic data provide
58 a foundation of understanding regarding the mycoremediation of PAHs
59 and the application of this strain for polluted environments.

60

61

62

63

64

65

66

67 **Keywords**

68 PAH (Polycyclic aromatic hydrocarbon), Mycoremediation, *Dentipellis* sp.

69 KUC8613, White rot fungus, Genomics, Transcriptomics

70 **INTRODUCTION**

71

72 Fungi play a major role as the decomposers of recalcitrant organic
73 matters in nature (de Boer et al. 2005). The potent degrading abilities of
74 fungi can be attributed to low specificity of catabolic enzymes and the
75 formation of mycelial networks that can enhance chemical bioavailability
76 (Harms, Schlosser and Wick 2011). Mycoremediation, which is based on
77 the use of fungi and mushrooms for the bioremediation of polluted areas,
78 is a promising method to remove many hazardous chemicals of
79 environmental and public health concern (Deshmukh, Khardenavis and
80 Purohit 2016).

81 Polycyclic aromatic hydrocarbons (PAHs) are a group of chemicals
82 with two or more fused aromatic rings of carbon and hydrogen atoms
83 (Kadri et al. 2017). Among the various toxic materials, PAHs has been one
84 of the major targets for mycoremediation due to their possible
85 carcinogenic and mutagenic risks (Mastrangelo, Fadda and Marzia 1996,
86 Schutzendubel et al. 1999). The high hydrophobicity and chemical stability
87 make them persistent in environments and cause bioaccumulation. While
88 PAHs can be naturally formed by forest fires or volcanic eruptions, the
89 incomplete combustion of organic materials during industrial and other
90 human activities account for the majority of PAH formation (Johansson and
91 van Bavel 2003). Several physical and chemical treatment methods
92 including incineration, UV oxidation, fixation, and solvent extraction have
93 been developed to remove PAHs, but they have many drawbacks since
94 they are not cost-effective and environment-friendly (Gan, Lau and Ng
95 2009). The biodegradation of PAHs using fungi and other microorganisms
96 has been regarded as an alternative method to remove PAHs without
97 causing significant ecological damages (Abe et al. 1995, Gran-Scheuch et
98 al. 2017).

99 It has been reported that many wood-degrading fungi can
100 efficiently degrade a wide variety of PAHs (Field et al. 1992). Both
101 ligninolytic and non-ligninolytic fungi can degrade PAHs with initial

102 oxidation of substrates but the metabolic pathways they use may differ
103 (Pozdnyakova 2012, Marco-Urrea, Garcia-Romera and Aranda 2015).
104 Ligninolytic fungi can produce extracellular ligninolytic enzymes including
105 manganese peroxidase (MnP), lignin peroxidase (LiP), and laccase to
106 produce quinone intermediates. Non-ligninolytic degradation of PAHs may
107 use intracellular cytochrome P450 monooxygenases (CYPs) to produce
108 unstable arene oxides which can be subsequently converted into phenols
109 or trans-dihydrodiols. It was previously reported that even some
110 ligninolytic fungi, including *Phanerochaete* and *Pleurotus* can use CYPs
111 instead of ligninolytic enzymes for PAH-degradation (Ghosal et al. 2016).

112 Although great efforts have been made to demonstrate PAH-
113 degradation in wood-degrading fungi through proteomic and metabolic
114 assays, whole genome and transcriptome studies have rarely been
115 conducted. A genome scale survey of potential PAH-responsive genes and
116 their regulation at transcriptional level can contribute to the
117 comprehensive understanding of complex genetic networks in a fungal
118 PAH-degradation system and identification of novel PAH-responsive genes
119 encoded in the genome.

120 *Dentipellis* sp. KUC8613, one of white rot fungi in the order
121 Russulales, has previously been screened by high tolerance to various
122 PAHs and regarded as a potential host for mycoremediation (Lee et al.
123 2014). In this study, we report the efficient PAH-removal by the KUC8613
124 strain over various PAHs. In order to expand our knowledge of the genetic
125 basis for the PAH-removal capability of this fungus, we sequenced and
126 analyzed the genome of *Dentipellis* sp. KUC8613 as part of the 1000
127 Fungal Genomes Project (1k FGP) (Grigoriev et al. 2014) at the US
128 Department of Energy Joint Genome Institute (JGI)
129 (<http://jgi.doe.gov/fungi>). From the genome, we investigated genetic
130 repertoires potentially involved in the metabolism of PAHs. We further
131 performed transcriptomic analysis to observe differential expression of
132 these genes by four different PAHs and to identify novel PAH-responsive
133 genes. Our genomic and transcriptomic analysis to elucidate PAH-removal

134 by KUC8613 will give us a more comprehensive understanding of PAH-
135 degradation by wood-degrading fungi.

136

137

138 **Materials and Methods**

139

140 **Fungal strains, chemicals, and media**

141 *Dentipellis* sp. KUC8613 was originally isolated from South Korea
142 and identified by the Korea University Culture collection (KUC). Anthracene
143 (ANT), fluoranthene (FLU), phenanthrene (PHE), pyrene (PYR), and all
144 solvents including ethyl acetate, chloroform, and acetonitrile were
145 purchased from Sigma (Sigma-Aldrich). Malt extract (ME) medium
146 contained 20 g malt extract for 1 liter distilled water. 15 g agar was
147 additionally added for malt extract agar (MEA) medium.

148

149 **Determination of tolerance to PAHs**

150 Four different PAHs (ANT, FLU, PHE, and PYR) were used to
151 determine tolerance of the fungus to PAHs. Fungal mycelia were cultured
152 on MEA containing 100 mg/liter of individual PAH. PAHs were first
153 dissolved in acetone prior to being added into the culture medium.
154 Acetone was evaporated from the medium by letting it stand for a few
155 days. An actively growing fungal disk was inoculated at the center of a
156 culture plate and incubated at 25 °C. Each sample was prepared in
157 triplicate and the growth rate of fungal mycelia was determined by
158 measuring the radius of the mycelia at between 0 and 10 days.

159

160 **Liquid culture condition and determination of mycelial growth**

161 Fungal mycelium was grown on MEA at 25 °C and maintained for
162 less than a week at 5 °C before use. Liquid ME containing 100 mg/liter of
163 individual PAH was prepared. PAHs were first dissolved in acetone and
164 added into ME medium. Acetone was evaporated from the medium by
165 letting it stand for a few days before fungal inoculation. An actively
166 growing mycelium disc (4 cm diameter) was homogenized for 10 seconds
167 in a sterile blender cup, containing 50 ml of ME medium. 2 ml of the
168 homogenate was used to inoculate 50 ml ME medium in a 250 ml
169 Erlenmeyer flask. Mycelium was grown at 25 °C in a rotary shaker with

170 shaking at 180 rpm. Heat-killed mycelia (400 mg in dry weight) and
171 cultures without fungal inoculation were also used for the determination of
172 PAH-adsorption to mycelia and natural degradation. Cultures were
173 incubated for between 0 and 10 days.

174 For the determination of mycelial growth during liquid culture,
175 mycelium was harvested after incubation by centrifugation and washed
176 twice with 50 ml distilled water to a final volume of 10 ml. The sample was
177 then and filtered through pre-weighted dried filter paper filter in a vacuum
178 filtration apparatus. The mycelium and filter paper were oven-dried at 65
179 °C for one day, and dry weight was measured.

180

181 **HPLC analysis of PAH-removal**

182 The dried extracts were dissolved in 1 ml chloroform. For the
183 quantitative analysis of residual PAHs, Waters high-pressure liquid
184 chromatography (HPLC) system (Milford, MA, USA) equipped with Waters
185 2487 UV detector was used. Data acquisition was carried out using the
186 Waters Empower 2 software. Ten microliters of each extract was injected
187 onto the Waters C18 column with a flow rate of 1 ml/min. The mobile
188 phase was acetonitrile : water (80:20) and the PAHs were detected at 254
189 nm.

190

191 **Genomic DNA extraction and sequencing**

192 The fungus was cultured on solid MEA media at 25 °C in the dark.
193 Genomic DNA was extracted from mycelium using a CTAB-based fungal
194 DNA isolation protocol (Fulton, Chunwongse and Tanksley 1995). The
195 concentration of prepared DNA was determined using Qubit fluorometer
196 (Invitrogen). For the whole genome sequencing of *Dentipellis* sp.
197 KUC8613, two Illumina libraries with insert sizes 5.5 kb and 370 bp were
198 prepared and sequenced using 2 × 150 bp reads from HiSeq-1TB. The
199 sequence data was filtered so as to remove low quality reads and
200 subsequently assembled with AllPathsLG release version R44008 (Gnerre
201 et al. 2011). The genome was annotated using the JGI Annotation Pipeline

202 (Grigoriev et al. 2014) and FunGAP (Min, Grigoriev and Choi 2017). From
203 JGI-MycoCosm repository
204 (<https://genome.jgi.doe.gov/Densp1/Densp1.home.html>), we could
205 retrieve the genome wide annotation data such as InterPro, CAZy, KOG,
206 and KEGG for functional analysis.

207

208 **RNA extraction and mRNA sequencing**

209 For transcriptomic analysis, RNA from 5 days of culture were used.
210 The grown mycelium was harvested from the culture medium by
211 centrifugation and washed twice with 50 ml distilled water. The mycelium
212 pellet was immediately frozen under liquid nitrogen and homogenized
213 using a mortar and a pestle. Total RNA was isolated using an RNeasy plus
214 mini kit (Qiagen, the Netherlands) according to the manufacturer's
215 protocol. RNA concentration was determined using Qubit fluorometer
216 (Invitrogen). RNA library was constructed using TruSeq RNA sample
217 preparation kit (Illumina, San Diego, CA, US). The sequencing of the RNA
218 library was carried out in MiSeq (2 × 200 cycles). Low-quality reads were
219 filtered using the Trim Galore program. The filtered RNA-seq data was
220 mapped against the assembled genome using CLC Genomics Workbench
221 software v.12.0 (Qiagen, the Netherlands). Read alignment was performed
222 with the following parameters: minimum length fraction and minimum
223 similarity fraction = 0.8, strand specific = both, maximum number of hits
224 for a read = 3. Reads Per Kilobase of transcript per Million mapped reads
225 (RPKM) value was generated using default settings of CLC genomics and
226 further used for the analysis of differential expression of genes. To check if
227 the RNA-seq data from different conditions correlate each other, a
228 Principal Component Analysis (PCA) was performed by an internal routine
229 of CLC Genomics Workbench.

230

231 **Gene Ontology enrichment analysis of upregulated genes**

232 Upregulated genes by PAHs were identified according to the
233 following criteria: fold change > 2 and p-value < 0.01. To further reveal

234 the enriched functions among upregulated genes, the Gene Ontology (GO)
235 enrichment analyses of upregulated genes were performed using the R
236 package clusterProfiler (version 3.2.1) (Yu et al. 2012). The threshold for
237 the enrichment analysis was p-value < 0.01.

238

239 **Results**

240

241 **PAH tolerance and removal capability by *Dentipellis* sp. KUC8613**

242 We measured the PAH tolerance of the fungus according to the
243 radial growth of mycelia in solid media (Fig. 1A). ANT, FLU, PHE, and PYR
244 were used as the representative PAHs having two to four fused aromatic
245 rings. The average growth rate of the fungus at 25 °C was 4.7 mm/day
246 without PAH. When four different PAHs were individually added in the
247 growth media, KUC8613 showed high tolerance to all four PAHs with
248 different degrees. In more detail, no detectable growth inhibition by ANT,
249 FLU, and PYR was observed at any time point within ten days. A moderate
250 decrease (14 %) in growth was observed only in PHE-added media. No
251 significant change in mycelial morphology or pigmentation by any of PAH
252 was recognized (Data not shown).

253 In order to verify PAH-removal by this fungus, the removal of PAHs
254 in liquid culture was examined (Fig. 2). HPLC-mediated quantification
255 showed that 44 % (ANT), 49 % (FLU), 33 % (PHE), and 46 % (PYR) of PAHs
256 were removed after five days. The removal of 90.1 % (ANT), 99 % (FLU),
257 94.3 % (PHE), and 94.4 % (PYR) of PAHs were observed after 10 days,
258 while 17.4 % (ANT), 25 % (FLU), 24.4 % (PHE), and 27.7 % (PYR) were
259 removed by autonomous chemical decomposition. We also observed that
260 less than 10 % of PAHs could be removed by adsorption to heat killed
261 mycelia. Fungal biomass (dry weight) in liquid culture was also measured
262 (Fig. S1). Only PHE induced a moderate growth retardation, which was
263 congruent with our observation in PAH tolerance test at solid media.

264

265 **Genome properties of *Dentipellis* sp. KUC8613**

266 In order to elucidate genetic contents for PAH-removal in this
267 fungus, whole genome sequencing was carried out under the 1k FGP
268 program. The genome sequence was 36.71 Mbp long, comprising 1,184
269 contigs and 425 scaffolds (Table 1). The GC content of the genome was
270 55.4 %. In total, 14,320 protein-coding genes were predicted in the

271 genome with an average gene length of 1,737 bp. Both the genome size
272 and the number of gene models of KUC8613 were typical among the
273 compared white rot fungi available from JGI mycosom (Grigoriev et al.
274 2014). Among 14,320 gene models, 6,305 (44 %) and 7,538 (52.6 %) were
275 assigned to different GO (Gene Ontology) terms and KOG (euKaryotic
276 Ortholog Groups) classes, respectively.

277 A genomic repository of carbohydrate-active enzymes (CAZymes)
278 was first surveyed in order to analyze the pattern of carbohydrate
279 metabolism in this fungus. The genome harbored a total of 417 CAZymes
280 including of 71 auxiliary activities (AA), 49 carbohydrate-binding modules
281 (CBM), and 180 glycoside hydrolases (GH) (Table S1). The cellulolytic
282 CAZyme composition in typical white rot fungi is generally represented by
283 the presence of lytic polysaccharide monoxygenases (LMPOs) (AA9),
284 cellobiohydrolases (GH6 and GH7), a single cellobiose dehydrogenase
285 (AA3-1), frequent CBM1-containing proteins, and ligninolytic enzymes
286 (Riley et al. 2014). Indeed, this strain revealed 11 copies of LMPOs that
287 potentially carry out the oxidative cleavage of polysaccharide chains
288 (Table S2). It also contained four cellobiohydrolases, 22 genes encoding
289 proteins carrying a CBM1 family module, and a single gene encoding
290 cellobiose dehydrogenase. The CAZyme-pattern suggests that *Dentipellis*
291 sp. KUC8613 has the classical wood decay mode of previously well-
292 characterized white rot fungi.

293 The genome of KUC8613 was annotated with 11 genes encoding
294 ligninolytic enzymes, including seven fungal class II peroxidases (PODs;
295 AA2) and four laccases (AA1_1). PODs were further classified into six MnPs
296 and a single LiP by sequence comparison. When we compared the
297 KUC8613 genome with eight other white rot fungal genomes, KUC8613
298 showed less than the average number of both PODs and laccase genes
299 among the compared genomes (Fig. 3).

300 While only a limited number of genes encoding ligninolytic enzymes
301 were found in the genome of KUC8613, we could instead identify other
302 genes encoding non-ligninolytic type of enzymes that can potentially

303 mediate the initial oxidation of aromatic ring structures. The presence of
304 154 putative P450s were revealed from the fungal genome (Table S3).
305 Using the Kyoto Encyclopedia of Genes and Genomes (KEGG) database
306 analysis, we could further sort out 77 P450s potentially involved in the
307 metabolism of xenobiotics, specifically those from CYP1, CYP2, and CYP3
308 families (Lewis 2003).

309 Additional genes that are potentially involved in the downstream
310 steps for PAH-transformation were also investigated (Table S4). We
311 identified 19 putative epoxide hydrolases that might catalyze a reaction to
312 produce trans-dihydrodiols from arene oxides. Oxidoreductase enzymes
313 including 16 alcohol dehydrogenases, 17 aldehyde dehydrogenases, one
314 trans-1,2-dihydrobenzene-1,2-diol dehydrogenase, and 31 FAD-dependent
315 monooxygenases may catalyze a series of oxidation reactions to produce
316 metabolic intermediates. Multicomponent dioxygenases comprising eight
317 ferredoxins, four ferredoxin reductases, two hydroxyquinol 1,2-
318 dioxygenases, and two aromatic ring-opening dioxygenases were also
319 found in the fungal genome. Aromatic intermediates formed by above
320 enzymes then can act as substrates for additional ring cleavage or
321 conjugation steps (Casillas et al. 1996, Habe and Omori 2003).
322 Glutathione S-transferases (GSTs), sulfotransferases, or
323 glycosyltransferases (GTFs) can catalyze the addition of glutathione,
324 sulfate, or glycosyl donors to PAH molecules, respectively, thus making
325 them less toxic and more water-soluble. In the genome of KUC8613, ten
326 putative GSTs, two sulfotransferases, and 13 GTFs were encoded for the
327 potential conjugation of PAH intermediates.

328

329 **Genome-wide transcriptomic responses during PAH removal**

330 In order to further investigate which of the potential genes are
331 actually upregulated during PAH-removal in this fungus, a genome-wide
332 transcriptomic analysis was performed. Mycelial discs grown for five days
333 in liquid ME media supplemented with ANT, FLU, PHE, and PYR (100
334 mg/liter) were subjected to RNA-seq. Principal component analysis (PCA)

335 of the gene expression data clearly separated PAH-added groups from the
336 control group (Fig. 4A). The PCA data also showed a separation within PAH
337 samples. While the ANT, FLU, and PYR samples were clustered together,
338 the PHE samples formed an independent group distinct from other PAH
339 samples, suggesting that the gene expression profile of PHE sample is
340 unlike those of other PAHs.

341 Of the 14,320 gene models predicted in the genome, we identified
342 1,922 genes whose expression was upregulated by at least one of four
343 different PAHs (Fold change > 2 and P-value < 0.01) (Table S5). The
344 numbers of total genes upregulated by ANT, FLU, PHE, and PYR were 915,
345 950, 1539, and 1,095, respectively (Fig. 4B). Among the upregulated
346 genes, the molecular function of 772 genes could not be predicted.
347 Upregulated genes were assigned to 23 specific KOG classes and
348 dominantly (54.9 % of 1,041 KOG-assigned genes) categorized into five
349 KOG classes including posttranslational modification, signal transduction,
350 energy production and conversion, carbohydrate transport and
351 metabolism, and transcription (Table S6). As illustrated by a Venn-diagram
352 in Figure 4B, upregulated genes showed common and different PAH-
353 specific overexpression during PAH-removal. A total of 550 genes were
354 commonly overexpressed by all four PAHs. The numbers of PAH-specific
355 genes by ANT, FLU, PHE, and PYR were 67, 72, 548, and 59, respectively.
356 The number of PHE-induced genes were significantly higher than genes
357 induced by other PAHs. A heatmap plotted by \log_2 RPKM of up-regulated
358 gene expression showed a similar pattern as well (Fig. 4C). The majority of
359 up-regulated genes were commonly overexpressed in all PAH-samples
360 while PHE showed a distinct gene expression pattern compared to those of
361 other three PAHs.

362 We first investigated the expression profiles of ligninolytic enzymes
363 (LiP, MnP, and laccase) and P450s for initial aromatic-ring oxidation. No
364 ligninolytic enzymes were upregulated during PAH-removal (Table S7). On
365 the other hand, P450s showed both common and different PAH-specific
366 overexpression. Among 154 putative P450 genes found in the KUC8613

367 genome, transcription of 15 genes was induced by one or more PAHs
368 (Table 2). Six P450 genes were constitutively upregulated by two or three
369 PAHs, while the remaining nine genes showed different PAH-specific
370 overexpression. These nine genes could be further categorized into six
371 PHE-inducible (ProtID 548471, 772453, 879478, 840982, 841965, and
372 873894) and one for each ANT-, FLU- or PYR-inducible genes (ProtID
373 861037, 798081, and 832704 for ANT, FLU, and PYR, respectively).

374 We also identified a total of 27 other PAH-responsive genes
375 potentially responsible for the downstream steps for PAH-transformation.
376 The expression patterns of these genes showed that most of them were
377 commonly overexpressed regardless of PAH-type (Fig. S2). These 27 PAH-
378 responsive genes were three epoxide hydrolases (ProtID 581771, 840197,
379 and 871191), three ferredoxins (ProtID 226033, 839077, and 887248), one
380 ferredoxin reductase (ProtID 832353), five alcohol dehydrogenases (ProtID
381 843873, 859290, 867273, 712202, and 886660), three aldehyde
382 dehydrogenases (ProtID 837250, 884278, and 857188), Five FAD-
383 dependent monooxygenases (ProtID 820609, 772612, 838248, 870155,
384 and 879414), two dioxygenases (ProtID 841503 and 842583), three GSTs
385 (ProtID 847321, 697729, and 830936), one GTF (ProtID 879011), and one
386 sulfotransferase (ProtID 838043).

387 In addition to the PAH-transforming genes, the 550 commonly
388 overexpressed genes by all four PAHs included 41 genes involved in lipid
389 transport and metabolism; these include a lipase (ProtID 835364), a sterol
390 desaturase (ProtID 864816), a methyltransferase (ProtID 833162), and a
391 phospholipid/glycerol acyltransferase (ProtID 39743) (Table S8). This
392 observation is consistent with previous studies in which the bioavailability
393 of hydrophobic PAHs can be enhanced by the cellular production of lipid
394 biosurfactants to emulsify PAHs and promote solubility (Cao et al. 2015).

395 Since our genomic and transcriptomic analysis suggests that this
396 fungus utilizes the intracellular non-ligninolytic type of enzymes instead of
397 extracellular ligninolytic enzymes for PAH-transformation, translocation of
398 PAHs and metabolic intermediates across the cell membranes and

399 organelles should be controlled by membrane bound transporters. It is
400 well known that major facilitator superfamily (MFS) transporters and ATP-
401 binding cassette (ABC) transporters are two major transporter families
402 that mediate the import and export of drugs and xenobiotics (Jeong et al.
403 2017, Carmona et al. 2009). We observed the common upregulation of 14
404 MFS and five ABC transporters by all four PAHs (Table S9). The active
405 transcription of MFS transporters was particularly noticeable by PHE. The
406 more than ten-fold elevated expression of four MFS transporters (ProtID
407 787334, 857773, 800757, and 328771) by PHE suggests an important role
408 of these transporters for cellular response to PHE.

409 While a significant number of genes were commonly overexpressed
410 by all four PAHs, certain genes also showed PAH-specificity within different
411 PAH-samples. Among four PAHs, PHE induced 35 % more genes than the
412 average number of upregulated genes by other PAHs. This resulted in the
413 PHE-specific overexpression of 548 genes (Fig. 4B). According to Gene
414 Ontology (GO) functional enrichment analysis, enriched GO terms among
415 PHE-specific genes were ATP synthesis coupled proton transport and
416 different types of cytochrome c oxidases (Fig S3). We also identified 10
417 additional MFS and two ABC transporters, suggesting their restricted
418 involvement in the translocation of PAHs other than PHE (Table S10). PAHs
419 are known to increase the production of reactive oxygen species (ROS),
420 leading to oxidative stress (Alkio et al. 2005). Since only PHE showed
421 detectable cytotoxicity during fungal growth, significant upregulation of
422 ROS scavenging enzymes is expected. Indeed, we observed the PHE-
423 specific upregulation of genes such as manganese and iron superoxide
424 dismutase (ProtID 648712, and 860732), and alkyl hydroperoxide
425 reductase (ProtID 194063), which are potentially involved in enzymatic
426 antioxidant defense mechanisms.

427

428 **Discussion**

429 PAH-transformation by wood-degrading fungi might be a ubiquitous
430 phenomenon (Field et al. 1992, Mao and Guan 2016). In this study, we
431 demonstrated that *Dentipellis* sp. KUC8613 have a high capability (> 90 %
432 of 100 mg/L PAH) of removing four different types of PAHs within a short
433 period of time. Our genomic and transcriptomic analysis to further
434 elucidate PAH-transforming system encoded in the genome revealed a
435 total of 1,922 upregulated genes many of which have unknown molecular
436 functions. To our knowledge, genome-scale transcriptomic responses by a
437 wood-degrading fungus during PAH-transformation have not been
438 previously described.

439 While ligninolytic system in white rot fungi was often described as
440 the key for PAH-transformation (Ghosal et al. 2016), our data showed that
441 KUC8613 was capable of removing PAHs using P450s instead of
442 ligninolytic enzymes. Ligninolytic enzymes may not be essential for PAH-
443 transformation in this fungi, but they still may take part in PAH-
444 transformation at certain growth conditions. It has been previously shown
445 that the production of ligninolytic enzymes by white rot fungi can be
446 dependent on carbon and nitrogen concentration in the growth media
447 (Ben Hamman, de La Rubia and Martinez 1997, D'Souza, Merrit and Reddy
448 1999). It would be worthwhile to check PAH-removal pattern by this
449 fungus under different conditions that favor the production of ligninolytic
450 enzymes. Taken together, these data strongly suggest that the screening
451 of strong mycoremediation hosts primarily based on ligninolytic enzyme
452 activities should be reconsidered.

453 Our transcriptomic analysis revealed that P450s might be
454 responsible for the initial oxidation of aromatic rings in this fungus. A
455 previous genome-scale identification of P450 genes in *Phanerochaete*
456 *chrysosporium* showed PAH-oxidizing activity of these enzymes with
457 varying PAH specificity (Syed et al. 2010). Similarly, upregulated P450s in
458 this fungus showed both PAH-specific and common overexpression
459 patterns. PHE induced the highest number of P450 genes, suggesting

460 metabolic complexity of this compound compared to other three PAHs. In
461 addition to P450s, we observed upregulation of many other genes
462 encoding potential PAH-transforming activities such as epoxide hydrolase,
463 alcohol dehydrogenase, aldehyde dehydrogenase, FAD-dependent
464 monooxygenase, dioxygenase, GTF, GST and sulfotransferase. The
465 biotransformation of PAHs by dioxygenases is mainly known to occur in
466 many PAH-degrading bacteria (Peng et al. 2008), but in some *Trichoderma*
467 species, involvement of dioxygenase was also reported during
468 phenanthrene degradation (Hadibarata, Tachibana and Itoh 2007). The
469 shared upregulation of many potential PAH-transforming genes suggests
470 some overlap between the metabolic pathways of different PAHs. The
471 elucidation of the exact molecular mechanisms associated with the key
472 enzymes discovered in this study requires further study. In addition,
473 upregulation of many genes with unknown molecular functions also gives
474 a clue for future research into the identification of novel genes involved in
475 PAH-transformation.

476 The distinct transcriptomic response induced by PHE in this fungus
477 was explained by a large number of PHE-specific genes involved in
478 translocation of PAHs, defense against ROS, and ATP synthesis. The reason
479 why PHE induced the transcription of a significantly larger number of
480 genes is not clear but our experimental evidences suggested that it might
481 be associated with PHE-induced cellular cytotoxicity. A similar observation
482 that PHE upregulated a larger number of genes than other PAHs was also
483 previously reported in soil fungus (Gao et al. 2019).

484 Based on the global gene expression pattern, we constructed a
485 tentative pathway for the transformation and detoxification of PAHs in
486 *Dentipellis sp.* KUC8613 (Fig. 5). The pathway includes the initial ring-
487 oxidation step followed by downstream transformation step as well as
488 transporters for the translocation of PAHs and their metabolites, lipases
489 for the enhanced solubility of PAHs, and antioxidant enzymes for reduced
490 oxidative stress. Our data based on whole-genomic and transcriptomic
491 analysis will provide a strong insight into the complex gene regulation of

492 wood-degrading fungi for PAH-degradation, and may serve as a guide for
493 the efficient screening and utilization of fungal hosts for mycoremediation.
494

495 **Accession numbers and availability of the genome sequence and**
496 **the strain**

497 This whole genome sequence of *Dentipellis* sp. KUC8613 has been
498 deposited at DDBJ/EMBL/GenBank under the accession number
499 NSJX00000000. In addition, the genome assembly and annotation are
500 available at DOE JGI Genome Portal MycoCosm (Grigoriev et al. 2014)
501 (<http://genome.jgi.doe.gov/Densp1>). The strain is available from Korean
502 Collection for Type Cultures (KCTC) with the accession number KCTC46678
503 (<http://kctc.kribb.re.kr/>)

504

505 **Acknowledgements**

506 This work is supported by the Cooperative Research Program for
507 Agriculture Science & Technology Development (Project No. PJ01337602)
508 Rural Development Administration and New and Renewable Energy Core
509 Technology Program of the Korea Institute of Energy Technology
510 Evaluation and Planning (KETEP) grants from the Ministry of Trade,
511 Industry and Energy (No. 20173010092460), Republic of Korea. The work
512 conducted by the U.S. Department of Energy Joint Genome Institute, a
513 DOE Office of Science User Facility, is supported by the Office of Science
514 of the U.S. Department of Energy under Contract No. DE-AC02-
515 05CH11231.

516

517

518 **References**

- 519 Abe, A., A. Inoue, R. Usami, K. Moriya & K. Horikoshi (1995) Degradation of
520 polyaromatic hydrocarbons by organic solvent-tolerant bacteria from
521 deep sea. *Biosci Biotechnol Biochem*, 59, 1154-6.
- 522 Alkio, M., T. M. Tabuchi, X. C. Wang & A. Colon-Carmona (2005) Stress
523 responses to polycyclic aromatic hydrocarbons in Arabidopsis
524 include growth inhibition and hypersensitive response-like
525 symptoms. *Journal of Experimental Botany*, 56, 2983-2994.
- 526 Ben Hamman, O., T. de La Rubia & J. Martinez (1997) Effect of carbon and
527 nitrogen limitation on lignin peroxidase and manganese peroxidase
528 production by *Phanerochaete flavido-alba*. *Journal of Applied*
529 *Microbiology*, 83, 751-757.
- 530 Cao, J., Q. Lai, J. Yuan & Z. Shao (2015) Genomic and metabolic analysis of
531 fluoranthene degradation pathway in *Celeribacter indicus* P73T. *Sci*
532 *Rep*, 5, 7741.
- 533 Carmona, M., M. T. Zamarro, B. Blazquez, G. Durante-Rodriguez, J. F.
534 Juarez, J. A. Valderrama, M. J. Barragan, J. L. Garcia & E. Diaz (2009)
535 Anaerobic catabolism of aromatic compounds: a genetic and
536 genomic view. *Microbiol Mol Biol Rev*, 73, 71-133.
- 537 Casillas, R. P., S. A. Crow, T. M. Heinze, J. Deck & C. E. Cerniglia (1996)
538 Initial oxidative and subsequent conjugative metabolites produced
539 during the metabolism of phenanthrene by fungi. *Journal of*
540 *Industrial Microbiology*, 16, 205-215.
- 541 D'Souza, T. M., C. S. Merrit & C. A. Reddy (1999) Lignin-modifying enzymes
542 of the white rot basidiomycete *Ganoderma lucidum*. *Applied and*
543 *Environmental Microbiology*, 65, 5307-5313.
- 544 de Boer, W., L. B. Folman, R. C. Summerbell & L. Boddy (2005) Living in a
545 fungal world: impact of fungi on soil bacterial niche development.
546 *Fems Microbiology Reviews*, 29, 795-811.
- 547 Deshmukh, R., A. A. Khardenavis & H. J. Purohit (2016) Diverse Metabolic
548 Capacities of Fungi for Bioremediation. *Indian J Microbiol*, 56, 247-
549 64.

550 Field, J. A., E. de Jong, G. Feijoo Costa & J. A. de Bont (1992)
551 Biodegradation of polycyclic aromatic hydrocarbons by new isolates
552 of white rot fungi. *Appl Environ Microbiol*, 58, 2219-26.

553 Fulton, T. M., J. Chunwongse & S. D. Tanksley (1995) Microprep Protocol for
554 Extraction of DNA from Tomato and Other Herbaceous Plants. *Plant*
555 *Molecular Biology Reporter*, 13, 207-209.

556 Gan, S., E. V. Lau & H. K. Ng (2009) Remediation of soils contaminated
557 with polycyclic aromatic hydrocarbons (PAHs). *Journal of Hazardous*
558 *Materials*, 172, 532-549.

559 Gao, R., D. C. Hao, W. L. Hu, S. Song, S. Y. Li & G. B. Ge (2019)
560 Transcriptome profile of polycyclic aromatic hydrocarbon-degrading
561 fungi isolated from *Taxus* rhizosphere. *Current Science*, 116, 1218-
562 1228.

563 Ghosal, D., S. Ghosh, T. K. Dutta & Y. Ahn (2016) Current State of
564 Knowledge in Microbial Degradation of Polycyclic Aromatic
565 Hydrocarbons (PAHs): A Review. *Front Microbiol*, 7, 1369.

566 Gnerre, S., I. MacCallum, D. Przybylski, F. J. Ribeiro, J. N. Burton, B. J.
567 Walker, T. Sharpe, G. Hall, T. P. Shea, S. Sykes, A. M. Berlin, D. Aird,
568 M. Costello, R. Daza, L. Williams, R. Nicol, A. Gnirke, C. Nusbaum, E.
569 S. Lander & D. B. Jaffe (2011) High-quality draft assemblies of
570 mammalian genomes from massively parallel sequence data.
571 *Proceedings of the National Academy of Sciences of the United*
572 *States of America*, 108, 1513-1518.

573 Gran-Scheuch, A., E. Fuentes, D. M. Bravo, J. C. Jimenez & J. M. Perez-
574 Donoso (2017) Isolation and Characterization of Phenanthrene
575 Degrading Bacteria from Diesel Fuel-Contaminated Antarctic Soils.
576 *Front Microbiol*, 8, 1634.

577 Grigoriev, I. V., R. Nikitin, S. Haridas, A. Kuo, R. Ohm, R. Otilar, R. Riley, A.
578 Salamov, X. Zhao, F. Korzeniewski, T. Smirnova, H. Nordberg, I.
579 Dubchak & I. Shabalov (2014) MycoCosm portal: gearing up for
580 1000 fungal genomes. *Nucleic Acids Res*, 42, D699-704.

581 Habe, H. & T. Omori (2003) Genetics of polycyclic aromatic hydrocarbon

582 metabolism in diverse aerobic bacteria. *Biosci Biotechnol Biochem*,
583 67, 225-43.

584 Hadibarata, T., S. Tachibana & K. Itoh (2007) Biodegradation of
585 phenanthrene by fungi screened from nature. *Pak J Biol Sci*, 10,
586 2535-43.

587 Harms, H., D. Schlosser & L. Y. Wick (2011) Untapped potential: exploiting
588 fungi in bioremediation of hazardous chemicals. *Nat Rev Microbiol*,
589 9, 177-92.

590 Jeong, C. B., D. H. Kim, H. M. Kang, Y. H. Lee, H. S. Kim, I. C. Kim & J. S. Lee
591 (2017) Genome-wide identification of ATP-binding cassette (ABC)
592 transporters and their roles in response to polycyclic aromatic
593 hydrocarbons (PAHs) in the copepod *Paracyclops nana*. *Aquat*
594 *Toxicol*, 183, 144-155.

595 Johansson, I. & B. van Bavel (2003) Levels and patterns of polycyclic
596 aromatic hydrocarbons in incineration ashes. *Sci Total Environ*, 311,
597 221-31.

598 Kadri, T., T. Rouissi, S. Kaur Brar, M. Cledon, S. Sarma & M. Verma (2017)
599 Biodegradation of polycyclic aromatic hydrocarbons (PAHs) by
600 fungal enzymes: A review. *J Environ Sci (China)*, 51, 52-74.

601 Lee, H., Y. Jang, Y. S. Choi, M. J. Kim, J. Lee, H. Lee, J. H. Hong, Y. M. Lee, G.
602 H. Kim & J. J. Kim (2014) Biotechnological procedures to select white
603 rot fungi for the degradation of PAHs. *J Microbiol Methods*, 97, 56-62.

604 Lewis, D. F. V. (2003) Human cytochromes P450 associated with the phase
605 1 metabolism of drugs and other xenobiotics: A compilation of
606 substrates and inhibitors of the CYP1, CYP2 and CYP3 families.
607 *Current Medicinal Chemistry*, 10, 1955-1972.

608 Mao, J. & W. W. Guan (2016) Fungal degradation of polycyclic aromatic
609 hydrocarbons (PAHs) by *Scopulariopsis brevicaulis* and its
610 application in bioremediation of PAH-contaminated soil. *Acta*
611 *Agriculturae Scandinavica Section B-Soil and Plant Science*, 66, 399-
612 405.

613 Marco-Urrea, E., I. Garcia-Romera & E. Aranda (2015) Potential of non-

614 ligninolytic fungi in bioremediation of chlorinated and polycyclic
615 aromatic hydrocarbons. *New Biotechnology*, 32, 620-628.

616 Mastrangelo, G., E. Fadda & V. Marzia (1996) Polycyclic aromatic
617 hydrocarbons and cancer in man. *Environmental Health*
618 *Perspectives*, 104, 1166-1170.

619 Min, B., I. V. Grigoriev & I. G. Choi (2017) FunGAP: Fungal Genome
620 Annotation Pipeline using evidence-based gene model evaluation.
621 *Bioinformatics*, 33, 2936-2937.

622 Peng, R. H., A. S. Xiong, Y. Xue, X. Y. Fu, F. Gao, W. Zhao, Y. S. Tian & Q. H.
623 Yao (2008) Microbial biodegradation of polyaromatic hydrocarbons.
624 *FEMS Microbiol Rev*, 32, 927-55.

625 Pozdnyakova, N. N. (2012) Involvement of the ligninolytic system of white-
626 rot and litter-decomposing fungi in the degradation of polycyclic
627 aromatic hydrocarbons. *Biotechnol Res Int*, 2012, 243217.

628 Riley, R., A. A. Salamov, D. W. Brown, L. G. Nagy, D. Floudas, B. W. Held, A.
629 Lévassieur, V. Lombard, E. Morin, R. Otiillar, E. A. Lindquist, H. Sun, K.
630 M. LaButti, J. Schmutz, D. Jabbour, H. Luo, S. E. Baker, A. G.
631 Pisabarro, J. D. Walton, R. A. Blanchette, B. Henrissat, F. Martin, D.
632 Cullen, D. S. Hibbett & I. V. Grigoriev (2014) Extensive sampling of
633 basidiomycete genomes demonstrates inadequacy of the white-rot/
634 brown-rot paradigm for wood decay fungi. *Proc Natl Acad Sci U S A*,
635 111, 9923-8.

636 Schützendübel, A., A. Majcherczyk, C. Johannes & A. Huttermann (1999)
637 Degradation of fluorene, anthracene, phenanthrene, fluoranthene,
638 and pyrene lacks connection to the production of extracellular
639 enzymes by *Pleurotus ostreatus* and *Bjerkandera adusta*.
640 *International Biodeterioration & Biodegradation*, 43, 93-100.

641 Syed, K., H. Doddapaneni, V. Subramanian, Y. W. Lam & J. S. Yadav (2010)
642 Genome-to-function characterization of novel fungal P450
643 monooxygenases oxidizing polycyclic aromatic hydrocarbons (PAHs).
644 *Biochemical and Biophysical Research Communications*, 399, 492-
645 497.

646 Yu, G. C., L. G. Wang, Y. Y. Han & Q. Y. He (2012) clusterProfiler: an R
647 Package for Comparing Biological Themes Among Gene Clusters.
648 *Omics-a Journal of Integrative Biology*, 16, 284-287.

649

650 **TABLES AND FIGURES LEGENDS**

651

652 Table 1. Genome features of *Dentipellis* sp. KUC8613 compared with other
653 white rot fungi

654 Table 2. Common and different PAH-specific upregulation of P450 genes
655 during PAH-removal

656 Figure 1. Radial growth of the fungal mycelia at the presence of different
657 PAHs. ANT, anthracene; FLU, fluoranthene; PHE, phenanthrene; PYR,
658 pyrene.

659 Figure 2. PAH-removal efficiency by *Dentipellis* sp. KUC8613. The residual
660 amount of PAH during the fungal culture was measured by HPLC. ANT,
661 anthracene; FLU, fluoranthene; PHE, phenanthrene; PYR, pyrene; Control
662 1, 10 days of incubation without fungal inoculation; Control 2, 10 days of
663 incubation with dead mycelia.

664 Figure 3. Comparison of relative tolerance to mixed PAHs (Lee et al., 2014)
665 and the number of ligninolytic enzymes in white rot fungi. The species
666 tree was built based on single-copy orthologs including *A. nidulans* as an
667 out-group. The bootstrap-based branch supports and the scale bar that
668 represents the mean number of amino acid substitutions per site are
669 shown. Gene numbers are shaded white or red based on the Z-scores
670 computed for each column.

671 Figure 4. Transcriptomic analysis during removal of four different PAHs. (A)
672 Principal component analysis (PCA) of transcriptomics data. (B) Venn-
673 diagram representing the number of upregulated genes by four different
674 PAHs. (C) Heatmap showing transcription pattern (\log_2 RPKM) of 1,922
675 upregulated genes by four different PAHs. Columns represent different
676 genes and rows represent different PAH-treated groups. ANT, anthracene;
677 FLU, fluoranthene; PHE, phenanthrene; PYR, pyrene.

678 Figure 5. A schematic view of PAH-transformation in *Dentipellis* sp.
679 KUC8613. Blue and Red arrows represent the common and PAH-specific

680 overexpression of PAH-transforming genes, respectively. The PAH-
681 transformation pathway was divided into 1) initial ring-oxidation, and 2)
682 downstream transformation steps based on key enzymatic reactions. ANT,
683 anthracene; FLU, fluoranthene; PHE, phenanthrene; PYR, pyrene.

684

685

686

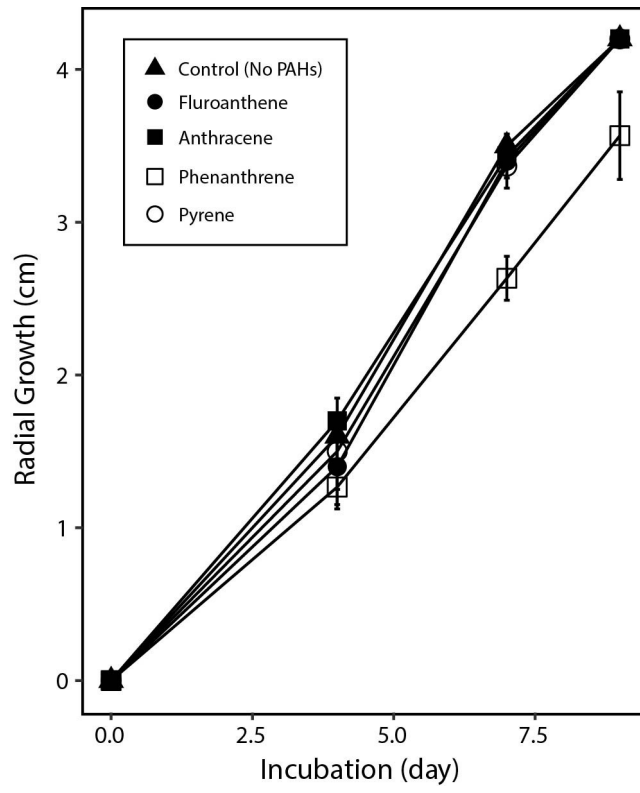
(Table 1)

Assembly statistics	<i>Dentipellis</i> sp. KUC8613	<i>H.</i> <i>annosum</i>	<i>T.</i> <i>versicolor</i>	<i>P. gigantea</i>	<i>B. adusta</i>	<i>P.</i> <i>brevispora</i> HHB-7030 SS6	<i>P.</i> <i>ostreatus</i> PC15	<i>S. paradoxa</i> KUC8140
Genome size (Mbp)	36.71	33.6	44.79	30.14	42.73	49.96	35.6	44.41
Number of contigs	1,184	630	1,443	1,195	1,263	3,178	3,272	1,374
Number of scaffolds	425	39	283	573	508	1,645	572	1,291
Annotation statistics								
Number of gene models	14,320	13,405	14,296	11,891	15,473	16,170	11,603	17,098
Average gene length (bp)	1,737	1,601	1,790	1,714	1,703	1,627	1,772	1,735
Average exon length (bp)	263	561	241	230	248	225	217	246
Average intron length (bp)	69	82	83	69	71	78	76	68
Average protein length (aa)	405	379	422	411	406	400	445	413
Number of exons per gene	5.47	5.39	5.81	6	5.59	5.66	6.4	5.78

(Table 2)

ProtID	Fold change ANT/ Control	P-value ANT/Contr ol	Fold change FLU/Contro l	P-value FLU/Contro l	Fold change PHE/Contr ol	P-value PHE/Contr ol	Fold change PYR/Contro l	P-value PYR/Contro l
859292	2.39*	1.00E-05	1.95	9.00E-04	2.59*	1.36E-06	2.63*	4.92E-07
882466	2.92*	8.40E-03	3.65*	1.30E-03	-	-	-	-
926550	-	-	2.13*	3.10E-03	-2.43	3.80E-03	2.03*	4.80E-03
833741	1.90	1.27E-05	2.13*	2.57E-07	2.78*	2.37E-12	2.05*	8.29E-07
818401	1.93	8.20E-03	3.04*	5.26E-06	2.62*	8.53E-05	2.27*	7.00E-04
875659	-	-	-	-	2.61*	1.99E-07	2.16*	2.54E-05
861037	2.19*	5.0E-04	1.91	5.10E-03	-	-	1.98	1.70E-03
798081	-	-	2.28*	3.30E-3	-	-	-	-
548471	-	-	-	-	2.55*	1.83E-11	-	-
772453	-	-	-	-	2.59*	3.60E-03	-	-
879478	1.73	2.60E-03	1.91	4.00E-04	3.17*	2.06E-10	1.91	4.00E-04
840982	-	-	-	-	2.69*	1.90E-03	-	-
841965	-	-	1.92	3.90E-3	2.99*	7.74E-07	-	-
873894	-	-	-	-	3.49*	9.90E-03	-	-
832704	-	-	1.73	2.00E-04	1.91	8.50E-06	2.07*	3.86E-07

688 Gene expression values with P-value > 0.01 were substituted by a dash (-). Fold changes of higher than 2 were bolded and denoted
689 with an asterisk (*).



690

691

692

(Fig. 1)

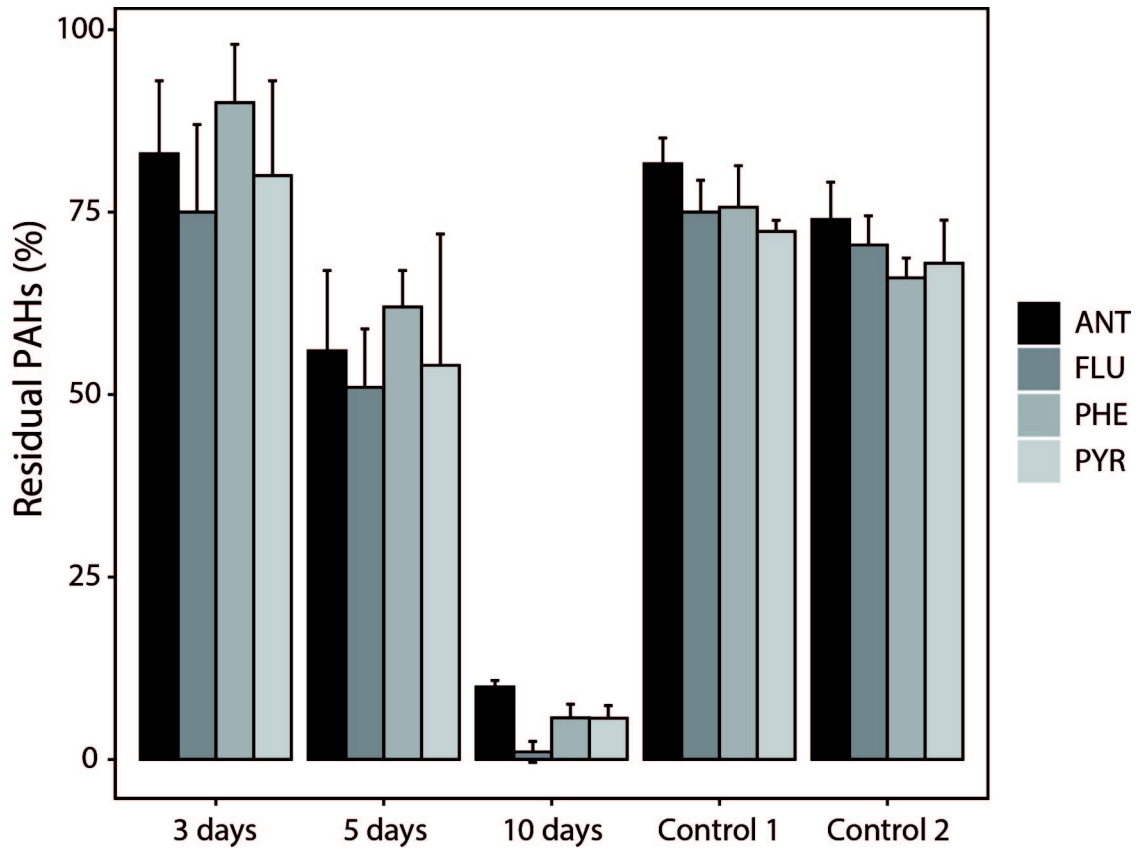
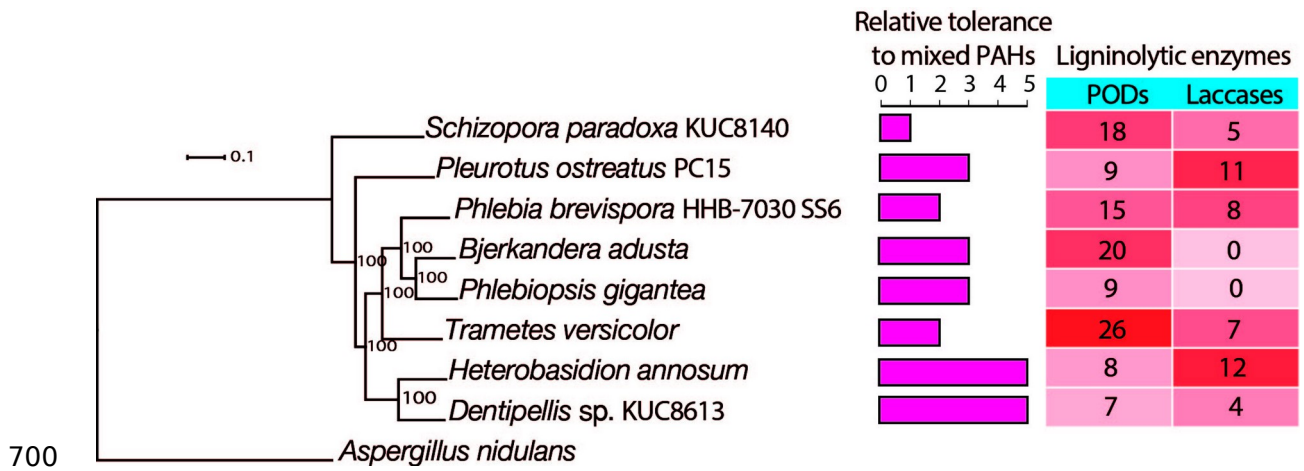


(Fig. 2)

693
 694
 695
 696
 697
 698
 699

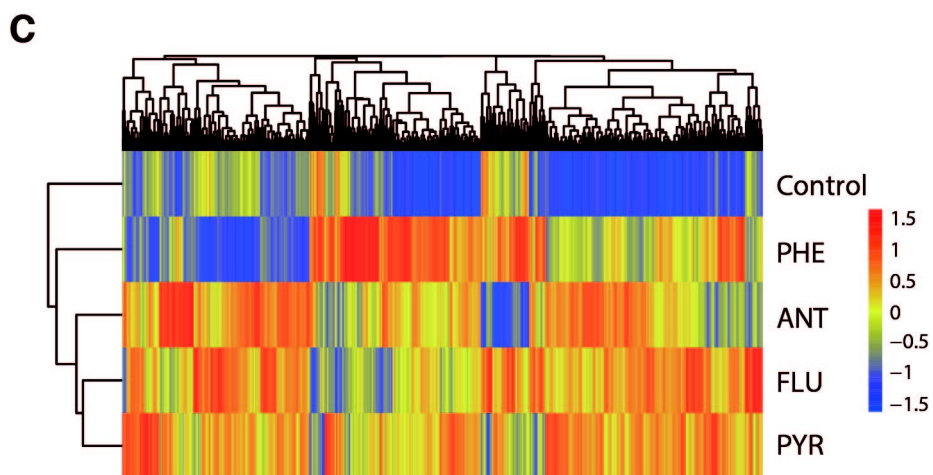
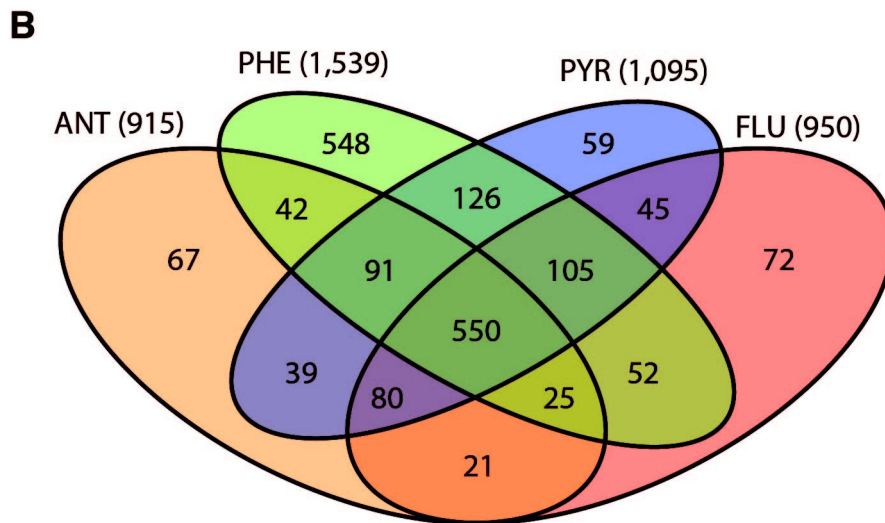
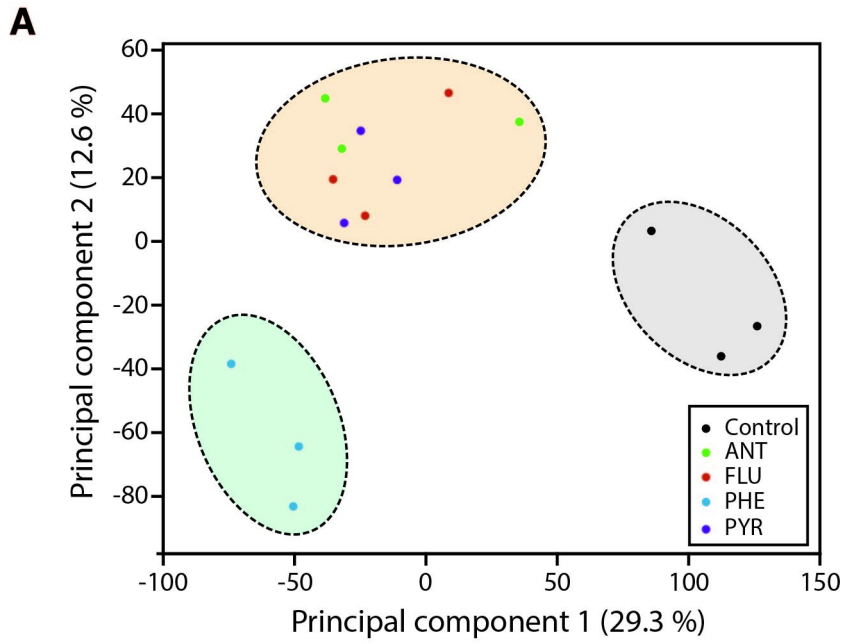


700

701

(Fig. 3)

702



703

704

(Fig. 4)

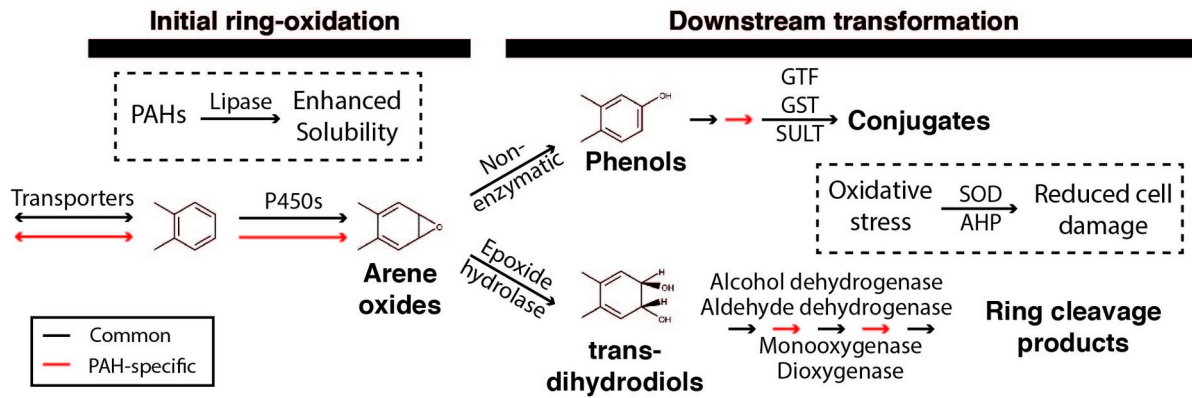


(Fig. 5)

705
706
707